Acta Cryst. (1993). B49, 367–374

Structural Comparison of Biologically Active and Inactive Conjugates of α-Amino Acids and the Plant Growth Hormone (Auxin) Indole-3-acetic Acid

BY BISERKA KOJIĆ-PRODIĆ,* BILJANA NIGOVIĆ, VITOMIR PUNTAREC, SANJA TOMIĆ AND VOLKER MAGNUS

Rudjer Bošković Institute, POB 1016, 41001 *Zagreb, Croatia*

(*Received* 14 *July* 1992; *accepted* 25 *September* 1992)

Abstract

The crystal structures of the naturally occurring biologically active conjugate *N*-(indol-3-ylacetyl)-L-valine [*N*-(IAA)-L-Val] and the synthetic inactive *N*-(indol-3-ylacetyl)-α-aminoisobutyric acid [*N*-(IAA)-α-Aib] have been determined. The growth-promoting activity of these compounds is discussed on the basis of their stereochemical properties. Conformational analysis of the amino-acid side chains has been performed by molecular mechanics and dynamics, and a comparison has been made with the conformations detected in the solid state. *N*-(IAA)-L-Val, $C_{15}H_{18}N_2O_3$, $M_r = 274.32$, monoclinic, $P2_1$, $a = 7.185$ (2), $b = 10.850$ (6), $c = 9.600$ (4) Å, $\beta = 105.80$ (4)°, $V = 720$ (1) Å^3, $Z = 2$, $D_x = 1.265$ g cm^{-3}, Cu $K\alpha$ radiation, $\lambda = 1.5418$ Å, $\mu = 6.902$ cm^{-1}, $F(000) = 292$, $T = 297$ K, $R = 0.052$, $wR = 0.059$ for 1452 reflections with $I \geq 3\sigma(I)$. *N*-(IAA)-α-Aib, $C_{14}H_{16}N_2O_3$, $M_r = 260.30$, monoclinic, $P2_1/c$, $a = 11.134$ (7), $b = 7.689$ (2), $c = 15.548$ (10) Å, $\beta = 95.62$ (3)°, $V = 1324$ (1) Å^3, $Z = 4$, $D_x = 1.311$ g cm^{-3}, Mo $K\alpha$ radiation, $\lambda = 0.71073$ Å, $\mu = 0.995$ cm^{-1}, $F(000) = 552$, $T = 297$ K, $R = 0.042$, $wR = 0.036$ for 1442 reflections with $I \geq 3\sigma(I)$. The indole ring system and the C atom of the adjacent methylene group are coplanar whereas the CON*R* residue adopts a folded conformation. In the structure of *N*-(IAA)-L-Val the peptide H faces the indole ring. In the structure of *N*-(IAA)-α-Aib the peptide group lies astride the ring plane and is involved in an intramolecular hydrogen bond to the carboxylic group. In both crystal structures packing is *via* N—H···O of the indole N atom and the carboxylic group, and O—H···O of the carboxylic group and peptide O atom.

Introduction

The plant hormone (auxin), indole-3-acetic acid (IAA), regulates physicological functions such as cell division and enlargement, development differentiation, and the synthesis of special proteins (Davies, 1987). The mechanism of auxin action is still the subject of debate and it is not fully understood how the hormone level in growing tissues is optimized. An important regulatory function has been ascribed to bound auxins, or auxin conjugates (Cohen & Bandurski, 1982; Magnus, 1987). These can be involved in IAA transport and can also serve as long- and short-term storage forms of the hormone, but a full elucidation of their physiology requires further research. Among the conjugates, several *N*-(indol-3-ylacetyl)amino acids have been isolated from plants and plant pathogens (*e.g.* Östin *et al.*, 1990; Epstein, Baldi & Cohen, 1986; Cohen, 1982; Hutzinger & Kosuge, 1968); others have been synthesized for comparative purposes (Wieland & Hörlein, 1955; Good, 1956; Mollan, Donelly & Harmey, 1972; Feung, Hamilton & Mumma, 1975; Hangarter, Peterson & Good, 1980; Magnus, Nigović, Hangarter & Good, 1992). In some cases, experimental evidence indicates that the auxin activity of these compounds depends on their conversion to the free growth hormone (Bialek, Meudt & Cohen, 1983; Hangarter & Good, 1981). However, direct oxidation of *N*-(IAA)-amino acids to biologically inactive metabolites has also been demonstrated (Park & Park, 1987; Tsurumi & Wada, 1986), while results of the interaction of free IAA and *N*-(IAA)-L-Ala in plant tissue culture (Hangarter, Peterson & Good, 1980; Magnus, Hangarter & Good, 1992) suggest that the conjugate *per se* may affect growth and development.

Molecular recognition of auxin and its biologically active conjugates has been studied (Kojić-Prodić, Nigović, Horvatić *et al.*, 1991; Kojić-Prodić, Nigović, Tomić *et al.*, 1991; Nigović, Kojić-Prodić & Puntarec, 1992; Nigović, Kojic-Prodić, Puntarec & Schagen, 1992). The significant difference in the growth-promoting property of *N*-(IAA)-L-Ala and *N*-(IAA)-D-Ala (Hangarter, Peterson & Good, 1980) provided the motive for a comparative structural analysis. This was extended to two further conjugates for which no crystallographic data were available: *N*-(IAA)-L-Val and *N*-(IAA)-α-Aib. *N*-(IAA)-L-Ala has been convincingly identified as an endogenous constituent in elongating shoots of *Picea abies* (Östin *et al.*, 1990); the L-valine conjugate has been found, by somewhat less conclusive methods, as

* To whom correspondence should be addressed.

0108-7681/93/020367-08$06.00

a metabolite of exogenous IAA in *Parthenocissus* crown gall tissues cultured *in vitro* (Feung, Hamilton & Mumma, 1976). In a set of ten α-amino-acid conjugates (see scheme below) tested as sources of auxin in plant tissue culture (Magnus, Nigović, Hangarter & Good, 1992) *N*-(IAA)-L-Ala was most active, *N*-(IAA)-L-Val moderately active, whereas the achiral *N*-(IAA)-α-Aib showed barely any activity.

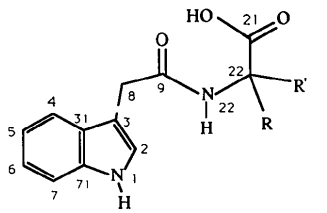

(1) *N*-(IAA)-Gly	R = H	R' = H
(2) *N*-(IAA)-L-Ala	R = CH_3	R' = H
(3) *N*-(IAA)-α-Aib	R = CH_3	R' = CH_3
(4) *N*-(IAA)-α-L-Abu	R = CH_2CH_3	R' = H
(5) *N*-(IAA)-L-Nva	R = $CH_2CH_2CH_3$	R' = H
(6) *N*-(IAA)-L-Nle	R = $CH_2CH_2CH_2CH_3$	R' = H
(7) *N*-(IAA)-L-Val	R = $CH(CH_3)_2$	R' = H
(8) *N*-(IAA)-L-Leu	R = $CH_2CH(CH_3)_2$	R' = H
(9) *N*-(IAA)-L-Ile	R = $CH(CH_3)CH_2CH_3$	R' = H
(10) *N*-(IAA)-DL-Asp	R = CH_2COOH	R' = H

Experimental

N-(IAA)-L-Val was prepared by the mixed-anhydride method as described by Wieland & Hörlein (1955) and Hangarter, Peterson & Good (1980). *N*-(IAA)-α-Aib may be prepared by the mixed-anhydride method with about 2% yield but the procedure described by Wang, Tam, Wang & Merrifield (1981) was used here (Magnus, Nigović, Hangarter & Good, 1992). Crystals of *N*-(IAA)-L-Val were obtained from 2-propanol and water (1:1 *v*/*v*) after 13 days at 275 (2) K. Crystals of *N*-(IAA)-α-Aib were grown from 2-propanol over 12 days at room temperature. Details of data collection and refinement are listed in Table 1. The molecule of *N*-(IAA)-L-Val is chiral (space group $P2_1$), and chirality was confirmed during refinement. The L-amino acid was used for the synthesis and the enantiomer with *S* configuration was selected for structure determination; the signs of the torsion angles are in accordance with this assignment.

Intensity data were collected on an Enraf–Nonius CAD-4F diffractometer with graphite-monochromatized radiation (Table 1). The measurements were carried out at room temperature for both compounds. No significant intensity variations were observed for standard reflections. Data were corrected for Lorentz and polarization effects using *SDP* (B. A. Frenz & Associates, Inc., 1982). An absorption correction was not applied. Structures were solved by *SHELX*86 (Sheldrick, 1985). Refinement was by full-matrix least-squares minimizing $\sum w(|F_o| - |F_c|)^2$ with the *SHELX*77 system of programs (Sheldrick, 1983) using *F* values. For the *N*-(IAA)-L-Val structure the H-atom coordinates for the pyrrole of the indole moiety, peptide and carboxylic groups were determined from successive difference Fourier syntheses. The H atoms attached to the benzene ring, C8, C23, C24 and C25 were calculated on stereochemical grounds and refined riding on their respective C atoms. The same procedure was used for *N*-(IAA)-α-Aib on C8 only. The N22—H bond distance in *N*-(IAA)-L-Val and N1—H in *N*-(IAA)-α-Aib were normalized to the value of 1.009 Å (Allen, Kennard & Watson, 1987). The O—H distance in the *N*-(IAA)-α-Aib structure was also normalized to the value of 0.95 Å. The non-H atoms were refined anisotropically; details of the refinement procedures are listed in Table 1. In the data set of *N*-(IAA)-L-Val the *y* coordinate of O9 was used to fix the origin in $P2_1$. Scattering factors are those included in *SHELX*77 (Sheldrick, 1983). Molecular geometry was calculated by the program package *EUCLID* (Spek, 1982). Drawings were prepared by *PLUTON* incorporated in *EUCLID* and *ORTEP*II (Johnson, 1976). The final atomic coordinates and equivalent isotropic thermal parameters are listed in Tables 2 and 3.*

Table 1. *Crystal data and summary of experimental details*

	N-(IAA)-L-Val	*N*-(IAA)-α-Aib
Molecular formula	$C_{15}H_{18}N_2O_3$	$C_{14}H_{16}N_2O_3$
M_r	274.32	260.30
Crystal size (mm)	0.30 × 0.150 × 0.20	0.36 × 0.25 × 0.14
a (Å)	7.185 (2)	11.134 (7)
b (Å)	10.850 (6)	7.689 (2)
c (Å)	9.600 (4)	15.548 (10)
β (°)	105.80 (4)	95.62 (3)
V (Å^3)	720 (1)	1324 (1)
Crystal system	Monoclinic	Monoclinic
Space group	$P2_1$	$P2_1/c$
D_x (g cm^{-3})	1.265	1.305
Z	2	4
μ (cm^{-1})	6.902 (Cu $K\alpha$)	0.868 (Mo $K\alpha$)
F(000)	292	552
T (K)	297	297
No. of reflections used for cell parameters and θ range (°)	25 6–17	25 9–14
θ range for intensity measurement (°)	2–25	2.5–25
hkl range	−8,8; −13,0; 0,11	0,13; 0,9; −18,18
$\omega/2\theta$ scan	0.8 + 0.35tanθ	0.8 + 0.35tanθ
No. of measured reflections	1715	2649
No. of unique reflections	1452	1442
R_{int}	0.0242	0.0131
	$I > 3\sigma(I)$	$I > 3\sigma(I)$
No. of variables	218	231
R	0.052	0.042
wR, $w^{-1} = k(\sigma F_o^2 + gF)$	0.059	0.036
S	0.26	0.67
k, g	1.00, 0.007	0.45, 0.016
Final shift/e.s.d	0.724 (C25, z)	0.156 (N22, x)
Residual electron density $(\Delta\rho)_{max}$, $(\Delta\rho)_{min}$ (e Å^{-3})	0.29, −0.28	0.16, −0.23

* Lists of structure factors, anisotropic thermal parameters and H-atom parameters have been deposited with the British Library Document Supply Centre as Supplementary Publication No. SUP 55669 (15 pp.). Copies may be obtained through The Technical Editor, International Union of Crystallography, 5 Abbey Square, Chester CH1 2HU, England.

Table 2. *Final atomic coordinates and equivalent isotropic thermal parameters* ($\times 10^4$) *for N-(IAA)-L-valine*

$U_{eq} = (1/3)\sum_i \sum_j U_{ij} a_i^* a_j^* \mathbf{a}_i . \mathbf{a}_j$.

	x	y	z	U_{eq} (Å^2)
N1	−0.1527 (2)	0.2717 (2)	0.6437 (2)	572 (1)
C2	−0.2933 (2)	0.3131 (2)	0.5265 (2)	524 (1)
C3	−0.2133 (2)	0.3956 (2)	0.4499 (2)	399 (1)
C31	−0.0113 (2)	0.4037 (2)	0.5258 (2)	378 (1)
C4	0.1414 (2)	0.4741 (2)	0.5057 (2)	498 (1)
C5	0.3211 (2)	0.4661 (2)	0.6055 (2)	660 (1)
C6	0.3512 (2)	0.3868 (2)	0.7230 (2)	698 (1)
C7	0.2051 (2)	0.3151 (2)	0.7463 (2)	640 (1)
C71	0.0209 (2)	0.3251 (2)	0.6470 (2)	453 (1)
C8	−0.3131 (2)	0.4648 (2)	0.3164 (2)	427 (1)
C9	−0.2733 (2)	0.4214 (2)	0.1773 (2)	354 (1)
O9	−0.3307 (2)	0.4809	0.0632 (2)	542 (1)
N22	−0.1746 (2)	0.3177 (2)	0.1814 (1)	352 (1)
C21	−0.2785 (2)	0.1719 (2)	−0.0247 (2)	349 (1)
C22	−0.1271 (2)	0.2637 (2)	0.0577 (2)	326 (1)
C23	0.0745 (2)	0.2029 (2)	0.1011 (2)	408 (1)
C24	0.0873 (2)	0.0982 (2)	0.2083 (2)	659 (1)
C25	0.2311 (2)	0.2984 (2)	0.1588 (2)	644 (1)
O211	−0.4114 (2)	0.1445 (2)	0.0405 (2)	505 (1)
O212	−0.2719 (2)	0.1297 (2)	−0.1393 (1)	498 (1)

Table 3. *Final atomic coordinates and equivalent isotropic thermal parameters* ($\times 10^4$) *for N-(IAA)-α-aminoisobutyric acid*

$U_{eq} = (1/3)\sum_i \sum_j U_{ij} a_i^* a_j^* \mathbf{a}_i . \mathbf{a}_j$.

	x	y	z	U_{eq} (Å^2)
N1	1.0087 (2)	0.7914 (3)	−0.0339 (2)	485 (10)
C2	0.8969 (3)	0.7210 (4)	−0.0591 (2)	459 (12)
C3	0.8531 (2)	0.6408 (3)	0.0090 (2)	385 (10)
C31	0.9416 (2)	0.6630 (3)	0.0808 (2)	403 (10)
C4	0.9500 (3)	0.6080 (5)	0.1674 (2)	590 (14)
C5	1.0529 (4)	0.6511 (5)	0.2201 (2)	771 (18)
C6	1.1462 (4)	0.7466 (5)	0.1900 (3)	681 (16)
C7	1.1407 (3)	0.8023 (4)	0.1059 (2)	545 (14)
C71	1.0385 (3)	0.7579 (3)	0.0522 (2)	400 (12)
C8	0.7355 (2)	0.5473 (4)	0.0115 (2)	466 (13)
C9	0.6561 (3)	0.6250 (4)	0.0755 (2)	430 (10)
O9	0.5906 (2)	0.5350 (2)	0.1176 (1)	571 (9)
N22	0.6609 (2)	0.7976 (3)	0.0826 (1)	384 (9)
C21	0.6380 (3)	1.0933 (3)	0.1201 (2)	359 (10)
C22	0.6000 (2)	0.9076 (3)	0.1419 (2)	332 (10)
C23	0.4629 (3)	0.8855 (5)	0.1274 (3)	505 (14)
C24	0.6481 (4)	0.8720 (5)	0.2355 (2)	522 (13)
O211	0.5644 (2)	1.2109 (3)	0.1446 (1)	572 (8)
O212	0.7289 (2)	1.1239 (2)	0.0863 (1)	481 (7)

Calculations were performed on MicroVAX II and IRIS-4D25G computers at the X-ray Laboratory, Rudjer Bošković Institute, Zagreb.

Molecular structures in the crystalline state

Interatomic distances, bond and selected torsion angles for *N*-(IAA)-L-Val and *N*-(IAA)-α-Aib are listed in Tables 4 and 5. The molecular structures are shown in Fig. 1. The data presented permit comparison of the molecular geometry of the naturally occurring highly active conjugates *N*-(IAA)-L-Val and *N*-(IAA)-L-Ala (Kojić-Prodić, Nigović, Horvatić *et al.*, 1991) with the inactive *N*-(IAA)-α-Aib. The geometry of the benzene part of the indole nucleus significantly deviates from that of a six-membered aromatic ring. Shortening of the C6—C7 bond [⟨1.371 (5)⟩ Å, mean value for the three structures presented in Table 4] and shrinkage of the C6—C7—C71 angle [⟨117.3 (3)⟩°, Table 4] were observed. Low- and room-temperature diffraction data for IAA (Kojić-Prodić, Puntarec & Nigović, in preparation; Chandrasekhar & Raghunathan, 1982, respectively) revealed the same effects. The values from low- and room-temperature experiments are C6—C7 = 1.378 (3), 1.373 (5) Å and C6—C7—C71 = 117.4 (2), 117.2 (3)°, respectively. Inspection of the Cambridge Structural Database (1991) yielded 144 structures containing an indole moiety, 73 of which had *R* values smaller than 0.07 and were selected for statistical analysis by *GSTAT*89 (Motherwell, Murray-Rust, Raftery, Allen & Doyle, 1989). Arithmetic means calculated from the data presented are 1.371 (13) Å for the length of the C6—C7 bond and 117.2 (7)° for the angle C6—C7—C71. In the amino-acid conjugates studied (Kojić-Prodić, Nigović, Horvatić *et al.*, 1991; Nigović, Kojić-Prodić & Puntarec, 1992; Nigović, Kojić-Prodić, Puntarec & Schagen, 1992) including those listed in Table 4, lengthening of the C9—O9 bond was observed to a mean value of 1.236 (4) Å, in contrast to a value of 1.210 (4) Å in the free auxin (Chandrasekhar & Raghunathan, 1982). This is a normal consequence of peptide bond formation.

In order to elucidate the essential structural parameters for biological activity of the bioactive conformer it should first be recognizable. For example, in the series of auxins the relevant conformational parameter is the orientation of the side chain with respect to the indole ring (Davies, 1987). The indole moiety and C atom of the adjacent methylene group are coplanar but the CON*R* residue can be either extended or folded. Structural studies of *N*-(IAA)-amino-acid conjugates indicate that the folded conformation predominates (Kojić-Prodić, Nigović, Horvatić *et al.*, 1991). The torsion angle C2—C3—C8—C9 is −106.8 (2)° for the valine conjugate and −120.5 (3)° for the α-aminoisobutyric acid conjugate, so that the amino-acid aliphatic backbone is brought closer to the benzene ring of the indole moiety (Fig. 1). In both active conjugates, *N*-(IAA)-L-Ala (Kojić-Prodić Nigović, Horvatić *et al.*, 1991) and *N*-(IAA)-Val, the amide nitrogen N22—H is orientated towards the indole ring and the conformation of the peptide bond is *trans*. However, *N*-(IAA)-α-Aib differs significantly in the conformation about the C22–C21 bond (Table 5, Fig. 2). The rotation about this bond makes possible the intramolecular hydrogen bond N22—H···O212 (Table 6) in the structure of *N*-(IAA)-α-Aib. The carboxylic group is oriented towards the benzene ring; the plane of the carboxylic group is almost perpendicular to the indole plane [86.2 (3)°]. In the structure of *N*-(IAA)-L-Val the carboxylic group and the peptide oxygen protrude from the main body of

Table 4. *Bond lengths* (Å) *and bond angles* (°) *for N-(IAA)-L-Val and N-(IAA)-α-Aib*

	N-(IAA)-L-Val	*N*-(IAA)-α-Aib
N1—C2	1.367 (2)	1.378 (4)
N1—C71	1.368 (2)	1.372 (4)
C2—C3	1.379 (3)	1.357 (4)
C3—C31	1.439 (2)	1.425 (4)
C3—C8	1.490 (3)	1.497 (3)
C31—C4	1.393 (3)	1.406 (4)
C31—C71	1.410 (3)	1.410 (4)
C4—C5	1.385 (2)	1.382 (5)
C5—C6	1.388 (3)	1.390 (6)
C6—C7	1.373 (3)	1.372 (6)
C7—C71	1.409 (2)	1.386 (4)
C8—C9	1.515 (3)	1.517 (4)
C9—O9	1.241 (2)	1.238 (4)
C9—N22	1.325 (3)	1.332 (4)
N22—C22	1.446 (3)	1.465 (3)
C21—C22	1.527 (3)	1.536 (3)
C22—C23	1.542 (2)	1.530 (4)
C22—C24		1.526 (4)
C23—C24	1.519 (3)	
C23—C25	1.519 (3)	
C21—O211	1.311 (3)	1.302 (4)
C21—O212	1.204 (2)	1.208 (4)
C2—N1—C71	110.2 (2)	109.2 (2)
N1—C2—C3	109.3 (1)	109.9 (3)
C2—C3—C8	127.8 (1)	128.3 (3)
C2—C3—C31	106.2 (2)	106.5 (2)
C31—C3—C8	126.0 (2)	125.2 (3)
C3—C31—C71	107.3 (1)	107.8 (3)
C3—C31—C4	133.4 (2)	133.7 (2)
C4—C31—C71	119.2 (2)	118.5 (3)
C31—C4—C5	119.4 (2)	118.0 (3)
C4—C5—C6	120.7 (2)	122.0 (3)
C5—C6—C7	121.8 (2)	121.4 (4)
C6—C7—C71	117.7 (2)	117.1 (3)
C31—C71—C7	121.2 (2)	123.1 (3)
N1—C71—C7	131.7 (2)	130.4 (3)
N1—C71—C31	107.1 (1)	106.6 (3)
C3—C8—C9	116.1 (2)	113.3 (2)
C8—C9—N22	117.8 (2)	115.2 (3)
C8—C9—O9	121.3 (2)	122.6 (3)
O9—C9—N22	121.0 (1)	122.3 (3)
C9—N22—C22	124.3 (1)	127.6 (2)
N22—C22—C21	113.3 (1)	104.1 (2)
N22—C22—C23	111.5 (1)	111.1 (2)
N22—C22—C24		110.9 (2)
C21—C22—C23	110.2 (2)	111.3 (2)
C21—C22—C24		107.4 (3)
C23—C22—C24		111.9 (3)
C22—C23—C24	112.5 (1)	
C22—C23—C25	110.8 (2)	
C24—C23—C25	111.2 (1)	
C22—C21—O211	114.2 (2)	112.7 (2)
C22—C21—O212	121.4 (2)	122.5 (2)
O211—C21—O212	124.4 (2)	124.8 (3)

Table 5. *Selected torsion angles* (°) *for N-(IAA)-L-Val and N-(IAA)-α-Aib compared with N-(IAA)-L-Ala*

	N-(IAA)-L-Val	*N*-(IAA)-α-Aib	*N*-(IAA)-L-Ala
C2—C3—C8—C9	−106.8 (2)	−120.5 (3)	−111.1 (4)
C3—C8—C9—O9	−171.6 (2)	−144.6 (3)	−172.7 (3)
C3—C8—C9—N22	8.3 (3)	36.1 (4)	6.6 (4)
C8—C9—N22—C22	179.3 (2)	−176.4 (2)	174.7 (3)
C9—N22—C22—C21	−91.2 (2)	−179.5 (3)	−76.2 (4)
C9—N22—C22—C23	143.9 (2)	−59.7 (4)	159.6 (3)
C9—N22—C22—C24		65.3 (4)	
N22—C22—C23—C24	61.6 (2)		
N22—C22—C23—C25	−63.5 (2)		
C21—C22—C23—C24	−65.1 (2)		
C21—C22—C23—C25	169.9 (2)		
N22—C22—C21—O211	−8.9 (2)	158.8 (2)	0.6 (4)
N22—C22—C21—O212	171.4 (2)	−23.4 (4)	179.9 (3)

the molecule and, together with the exposed indole NH, converge relatively well into a hydrophilic pole, thus imposing amphipathic character upon the molecule. This is less pronounced in the α-Aib conjugate, as the different orientation of the carboxylic group leads to a more diffuse arrangement of hydrophilic structural elements.

Crystal packing

Diagrams illustrating the packing of *N*-(IAA)-L-Val and *N*-(IAA)-α-Aib in the crystal lattice *via* intermolecular hydrogen bonds are given in Figs. 3 and 4. In both cases tetramers are formed by hydrogen bonds between peptide oxygen atoms and carboxylic groups [O211—H···O9 (Table 6)] and between the indole nitrogen and carboxylic C=O groups (N1—H···O212). In the structure of *N*-(IAA)-L-Val, tetramers are joined into a three-dimensional network by a 2_1 symmetry operation and translation along **c** (Fig. 3). The same crystal-packing pattern has been observed for other amino-acid conjugates with $P2_1$ space-group symmetry (Kojić-Prodić, Nigović, Hor-

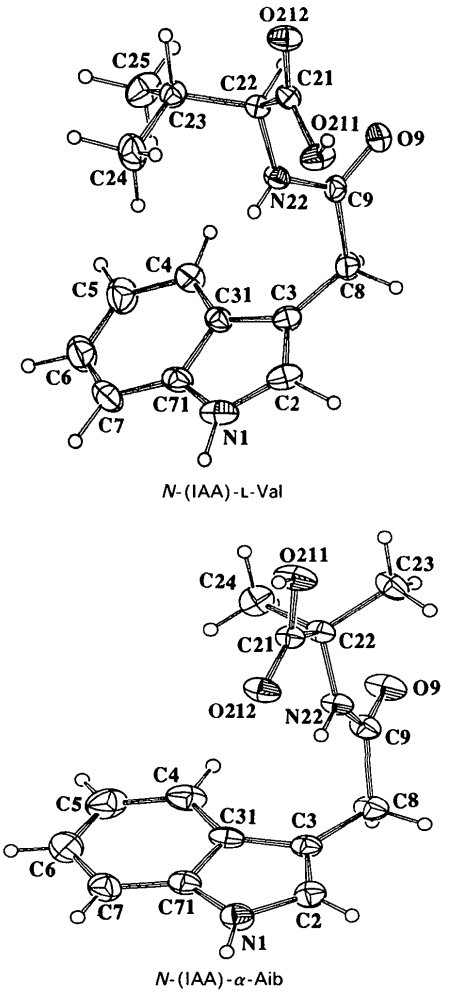

Fig. 1. Molecular structures (*ORTEP* drawings) and atom numbering of *N*-IAA-L-Val and *N*-(IAA)-α-Aib. The thermal ellipsoids are drawn at the 50% probability level.

Table 6. *Hydrogen bonds*

		D—H···*A* (Å)	*D*—H (Å)	H···*A* (Å)	*D*—H···*A* (°)	Symmetry operations on *A*
N-(IAA)-L-Val	N1—H···O212	2.901 (3)	0.98 (3)	1.94 (3)	166 (2)	$x, y, z+1$
	O211—H···O9	2.563 (2)	0.96 (3)	1.70 (2)	148 (2)	$-x-1, y-\frac{1}{2}, -z$
N-(IAA)-α-Aib	N1—H···O212	3.175 (3)	1.01 (3)	2.31 (3)	143 (2)	$-x+2, -y+2, -z$
	O211—H···O9	2.547 (3)	0.98 (4)	1.59 (4)	163 (3)	$x, y+1, z$

vatić *et al.*, 1991). The achiral molecule of *N*-(IAA)-α-Aib crystallizes in $P2_1/c$ but the packing pattern is completely different from that of other conjugates appearing in the same space-group symmetry. The IAA molecule (Chandrasekhar & Raghunathan, 1982) and other achiral conjugates (Kojić-Prodić, Nigović, Horvatić *et al.*, 1991) crystallize in the space group $P2_1/c$ with hydrogen-bonded dimers *via* carboxylic groups through the centre of inversion. However, the different orientation of the carboxylic group in the structure of *N*-(IAA)-α-Aib disables O—H···O interaction. Instead, dimers through the inversion centre are joined by hydrogen bonds N1—H···O212 (Table 6, Fig. 4). The hydrogen bond O211—H···O9 completes a tetramer which is the basic structural unit of a spiral running along **b**.

Molecular mechanics and dynamics calculations

To recognize the energetically optimized conformers of *N*-(IAA)-L-Val, *N*-(IAA)-α-Aib and, for comparison, *N*-(IAA)-L-Ala, molecular mechanics based on the consistent valence force-field approach of Lifson & Warshel (1969), Hagler, Huler & Lifson (1974) and Hagler, Lifson & Dauber (1979) incorporated in the program *DISCOVER*, version 2.7.0 (Biosym Technologies, 1991) was used. Molecular-mechanics optimizations were accomplished by steepest descent and conjugate gradient, and in some cases modified Newton–Raphson algorithms were used. Energy optimization was performed using the atomic coordinates from X-ray analysis (Tables 2 and 3, Kojić-Prodić, Nigović, Horvatić *et al.*, 1991) considering: (*a*) the molecule in the crystal lattice, *i.e.* using periodic boundary conditions, and (*b*) treating it as an isolated molecule '*in vacuo*' (gas phase). Conformation analysis of the amino-acid side chain was performed for four torsion angles (Table 7) which define: (*a*) the relative orientation of the entire side chain towards the indole plane (C2—C3—C8—C9); (*b*) the orientation of the peptide carbonyl (C3—C8—C9—O9); (*c*) the conformation about the bond linking the peptide moiety to the chiral (or prochiral) centre (C9—N22—C22—C21); and (*d*) the orientation of the carboxylic group (N22—C22—C21—O212). For the above molecules, the folded shape observed in the solid state (X-ray analysis) was, in

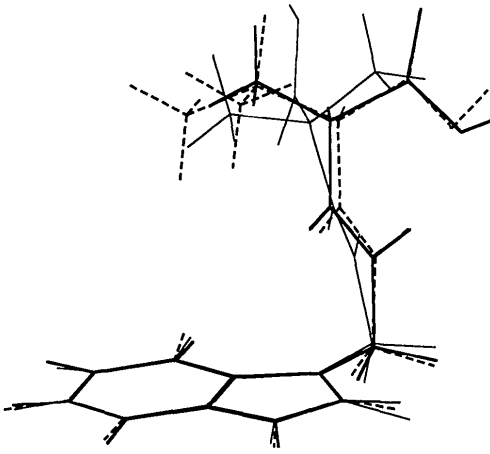

Fig. 2. The overlap of crystallographically observed conformations of *N*-IAA-L-Ala (heavy line), *N*-IAA-L-Val (dashed line) and *N*-(IAA)-α-Aib (light line).

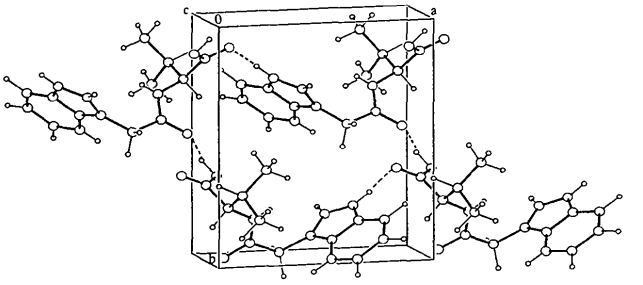

Fig. 3. Molecular packing of *N*-IAA-L-Val.

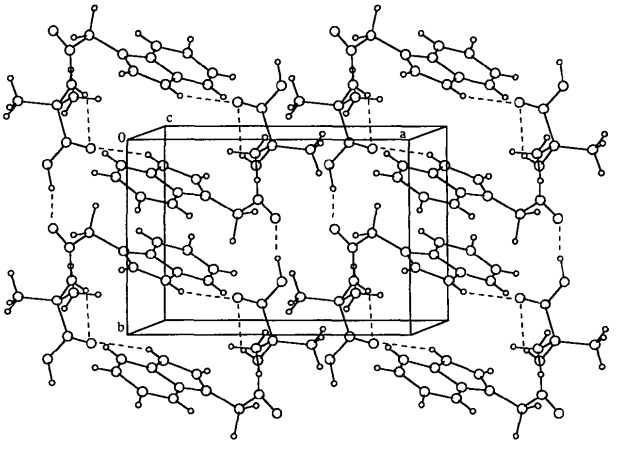

Fig. 4. Molecular packing of *N*-(IAA)-α-Aib.

Table 7. *Conformation analysis of an amino-acid side chain*

Torsion angles (°) obtained by X-ray analysis (first entry), molecular-mechanics energy optimization of the molecule in periodic boundary conditions (second entry), in gas phase (third entry), and in solution ^{1}H NMR* (fourth entry).

	C2—C3—C8—C9				C3—C8—C9—O9				C9—N22—C22—C21				N22—C22—C21—O212			
N-(IAA)-L-Ala	−111.1	−102	−115	−80 ± 10†	−172.7	177	−103	0, 180	−76.2	−78	−81	−80	−179.9	180	123	
N-(IAA)-L-Val	−106.8	−103	−125		−171.6	177	−118		−91.2	−81	−115		171.4	153	135	
N-(IAA)-α-Aib	−120.5	−122	−128		−144.6	−131	−115		−179.5	176	177		−23.4	−37	−3	

* Values were taken from Duddeck *et al.* (1989).
† Signs are derived from the molecular model.

global terms, conserved in the optimized conformations. Those obtained by the optimization procedure with the molecule in the periodic boundary conditions are close to those established by X-ray structure analysis (Table 7). However, the optimization procedure with isolated molecules (in the gas phase) revealed conformations about the C8—C9 and C22—C21 bonds different from those observed by X-ray structure analysis. Significant differences occurred for the orientation of the peptide and carboxylic groups. In the crystalline state the peptide oxygen of *N*-(IAA)-L-Ala and *N*-(IAA)-L-Val is pointing away from the indole plane having a (−)antiperiplanar conformation (Klyne & Prelog, 1960) about the C8—C9 bond (Table 7, Fig. 5). However, in the optimized conformer (in the gas phase) the peptide group lies astride the indole plane as is the case for the inactive *N*-(IAA)-α-Aib in the crystal as well as in the gas phase (Table 7, Fig. 5); the conformation about C8—C9 is (−)anticlinal. A conformational search on the *N*-(IAA)-α-Aib molecule performed by rotation about the C22—C21 bond detected three rotamers of nearly equal energy (difference < 2.1 kJ mol^{-1}) with torsion angles 0, 179 and −148°. Generally, for the compounds studied (Table 7) the conformations observed in the solid state and those obtained by molecular-mechanics optimization are of three categories. The plane of the COOH group may be perpendicular to the N22—C22 bond [(+)anticlinal conformation about the C22—C21 bond] or parallel to it [(−)synperiplanar and (±)antiperiplanar conformations]. In solution, at physiological pH, the carboxylic group is deprotonated and a 180° rotation does not result in a new conformer. The biologically active *N*-(IAA)-L-Ala and *N*-(IAA)-L-Val showed (±)antiperiplanar conformations in the crystalline state, but (+)anticlinal conformation in the optimized conformers (in the gas phase). For *N*-(IAA)-α-Aib the orientations of the carboxylic group in the solid state and in the optimized molecule in the gas phase were not significantly different. Simulation of the molecular conformation of *N*-(IAA)-L-Ala on the *N*-(IAA)-α-Aib molecule already optimized by molecular mechanics ended with a conformation close to that obtained by the minimization of the original *N*-(IAA)-α-Aib X-ray conformer.

Discussion

A number of *N*-(indol-3-ylacetyl)amino acids have been tested as sources of auxin in tissue culture systems such as tomato hypocotyl explants and tobacco and *Solanum nigrum* callus (Hangarter, Peterson & Good, 1980; Magnus, Nigović, Hangarter & Good, 1992). The response to those conjugates varied widely depending on the amino-acid moiety. This has been ascribed to differences in uptake, in sensitivity to degradation by peroxidases (Park & Park, 1987) and (di)oxindole-forming enzymes (Tsurumi & Wada, 1986), in the rates of hydrolysis to free IAA (Hangarter & Good, 1981),

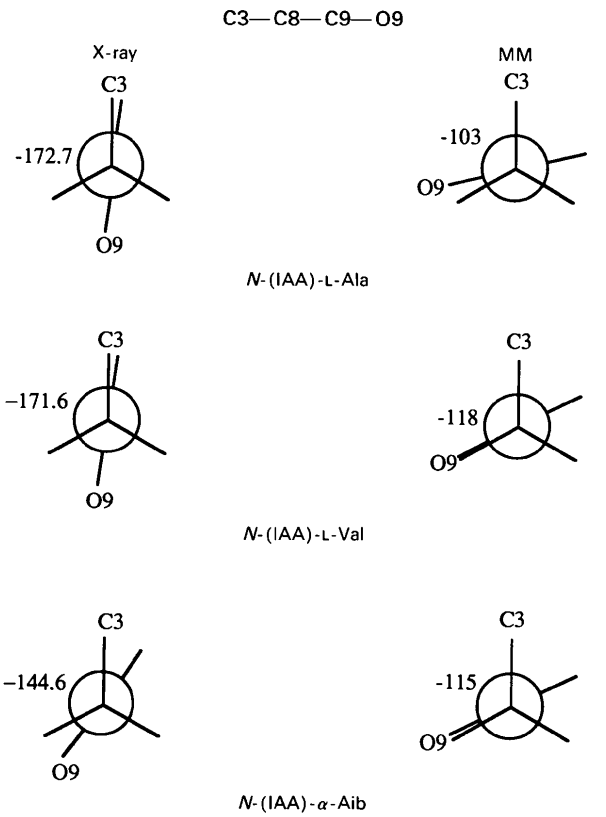

Fig. 5. Newman projections about the C8—C9 bond illustrate distinct orientations of peptide oxygen in the crystalline state and optimized conformers in a gas phase.

and in *per se* bioactivity of the conjugates (Hangarter, Peterson & Good, 1980; Magnus, Hangarter & Good, 1992). The relative significance of these factors appears to be tissue dependent and so far can not be analyzed in all its complexity. However, at least for tomato hypocotyl explants, experimental evidence suggests that most of the differences in the overall growth-promoting activities of IAA-amino-acid conjugates (not necessarily all subtle effects on organogenesis) are correlated to their rates of hydrolysis to the free hormone (Hangarter, Peterson & Good, 1980; Hangarter & Good, 1981). We focus therefore, on this aspect in an attempt to rationalize the drastic difference in activity between *N*-(IAA)-L-Ala and *N*-(IAA)-L-Val on one hand, and *N*-(IAA)-D-Ala and *N*-(IAA)-α-Aib on the other.

Hydrolase activity towards the L-alanine conjugate has, in fact, been demonstrated in bean internodes, but not charcterized in sufficient detail (Bialek & Cohen, 1984). Generally, *N*-acylamino acids are cleaved by some proteases, mostly carboxypeptidases and acylases, which have been isolated from a variety of microorganisms and from plant and animal tissues (Hanson, 1966; Lorand, 1976; Fersht, 1977; McDonald & Barrett, 1986). While the organization of the active sites in these enzymes varies in many details, the evidence available so far suggests that the following structural features are usually important: (*a*) a catalytic centre which cleaves the peptide bond and (*b*) auxiliary sites which interact with other topological elements of the peptide thus contributing to substrate and chiral specificity. For example, in the particularly well studied carboxypeptidase A from bovine pancreas (*i.e.* Fersht, 1977), an arginine (Arg145) residue functions as an auxiliary site in the above sense in that it binds the C-terminal carboxyl group of the substrate. This is essential (peptides lacking that group are not hydrolyzed) for proper alignment of the adjacent peptide bond with the catalytic centre consisting, in this particular case, of (1) complexed Zn^{2+} which binds the carbonyl oxygen and (2) a glutamine (Glu270) carboxylate ion and a tyrosine (Tyr248) hydroxyl group which then cleave the peptide bond by concerted acid–base catalysis. Comparative conformational analysis of *N*-(IAA)-α-Aib and the two biologically active conjugates (Table 7, Fig. 6) revealed obvious differences concerning the preferred rotamer of the carboxyl group with respect to the C21—C22 bond. This can, however, be of little significance for affinity to a carboxyl-recognizing auxiliary binding site of a plant peptidase, which would be expected to function at a pH at which the carboxyl group of IAA-amino-acid conjugates are dissociated (deprotonized). The two O atoms present would thus be equivalent, and a half-turn (approximately) about C21—C22 would not lead to a substantially different conformation. The difference between *N*-(IAA)-α-Aib and the two biologically active conjugates concerning the dihedral angle C9—N22—C22—C21 should, however, influence alignment of the peptide bond with the catalytic centre and thus the rate of hydrolysis. Inverse configuration at the chiral centre of *N*-(IAA)-Ala (Fig. 6) should have a similar effect. For instance, both carboxypeptidase A and acylase I from hog kidneys can cleave certain *N*-acyl-D-alanines, but at a much lower rate than their L-isomers (Hanson, 1966). Thus it is interesting to note that *N*-(IAA)-D-Ala is not completely devoid of biological activity, but supports growth in plant tissue culture to a much lesser extent than its L-isomer (Hangarter, Peterson & Good, 1980). In *N*-(IAA)-α-Aib substitution of C22 by two methyl groups appears to impose steric hindrance on the interaction of the neighbouring peptide NH with the catalytic centre of the hydrolyzing enzyme. Acylase I from hog kidneys cleaves *N*-acetyl-α-Aib and *N*-acetyl-D-Ala at about the same very slow rate (Hanson, 1966).

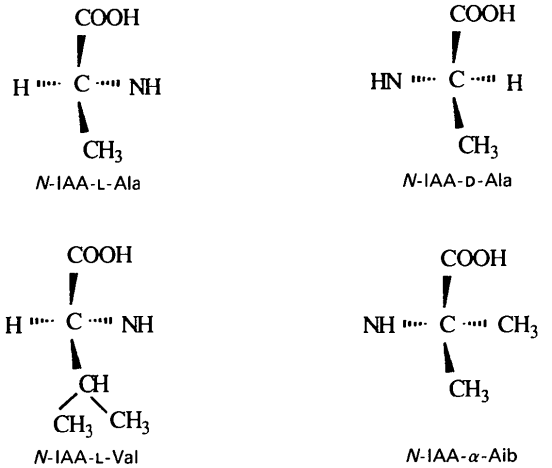

Fig. 6. The environments of chiral centres (C22) in the biologically active analogues *N*-(IAA)-L-Val, *N*-(IAA)-L-Ala, and inactive D-Ala conjugate with prochiral centre in the inactive *N*-(IAA)-α-Aib.

The project was partly supported by the Ministry of Science, Technology and Informatics, Republic of Croatia. The authors thank Professor Jan Kroon, University of Utrecht, The Netherlands, for valuable comments.

References

ALLEN, F. A., KENNARD, O. & WATSON, D. G. (1987). *J. Chem. Soc. Perkin Trans.* 2, pp. S1–S19.

B. A. FRENZ & ASSOCIATES, INC. (1982). *SDP Structure Determination Package*. College Station, Texas, USA.

BIALEK, K. & COHEN, J. D. (1984). *Plant Physiol. (Suppl.)* **75**, 108.

BIALEK, K., MEUDT, W. & COHEN, J. D. (1983). *Plant Physiol.* **73**, 130–134.

Biosym Technologies (1991). *DISCOVER*. Version 2.7.0. Biosym Technologies, 10065 Barnes Canyon Rd, San Diego, CA 92121, USA.

Cambridge Structural Database. (1991). Version 4. Cambridge Crystallographic Data Centre, Univ. Chemical Laboratory, Cambridge, England.

CHANDRASEKHAR, K. & RAGHUNATHAN, S. (1982). *Acta Cryst.* B**38**, 2534–2535.

COHEN, J. D. (1982). *Plant Physiol.* **70**, 749–753.

COHEN, J. D. & BANDURSKI, R. S. (1982). *Annu. Rev. Plant Physiol.* **33**, 403–430.

DAVIES, P. J. (1987). *Plant Hormones and Their Role in Plant Growth and Development*. Dordrecht: Martinus Nijhoff.

DUDDECK, H., HIEGEMANN, M., SIMEONOV, M. F., KOJIĆ-PRODIĆ, B., NIGOVIĆ, B. & MAGNUS, V. (1989). *Z. Naturforsch. Teil C*, **44**, 543–554.

EPSTEIN, E., BALDI, B. G. & COHEN, J. D. (1986). *Plant Physiol.* **80**, 256–258.

FERSHT, A. (1977). *Enzyme Structure and Mechanism*. San Francisco: W. H. Freeman.

FEUNG, C. S., HAMILTON, R. H. & MUMMA, R. O. (1975). *J. Agric. Food Chem.* **23**, 1120–1124.

FEUNG, C. S., HAMILTON, R. H. & MUMMA, R. O. (1976). *Plant Physiol.* **58**, 666–669.

GOOD, N. E. (1956). *Can. J. Chem.* **34**, 1356–1358.

HAGLER, A. T., HULER, Z. & LIFSON, S. (1974). *J. Am. Chem. Soc.* **98**, 5319–5327.

HAGLER, A. T., LIFSON, S. & DAUBER, P. (1979). *J. Am. Chem. Soc.* **101**, 5122–5130.

HANGARTER, R. P. & GOOD, N. E. (1981). *Plant Physiol.* **68**, 1424–1427.

HANGARTER, R. P., PETERSON, M. D. & GOOD, N. E. (1980). *Plant Physiol.* **65**, 761–767.

HANSON, H. (1966). *Peptidasen (Exopeptidasen)*. In *Handbuch der physiologisch- und pathologisch-chemischen Analyse. Enzyme*, Part C, edited by K. LANG & E. LEHNARTZ. Berlin: Springer-Verlag.

HUTZINGER, O. & KOSUGE, T. (1968). *Biochemistry*, **7**, 601–605.

JOHNSON, C. K. (1976). *ORTEP*II. Report ORNL-5138. Oak Ridge National Laboratory, Tennessee, USA.

KLYNE, W. & PRELOG, V. (1960). *Experientia*, **16**, 521–568.

KOJIĆ-PRODIĆ, B., NIGOVIĆ, B., HORVATIĆ, D., RUŽIĆ-TOROŠ, Ž., MAGNUS, V., DUAX, W. L., STEZOWSKI, J. J. & BRESCIANI-PAHOR, N. (1991). *Acta Cryst.* B**47**, 107–115.

KOJIĆ-PRODIĆ, B., NIGOVIĆ, B., TOMIĆ, S., ILIĆ, N., MAGNUS, V., KONJEVIĆ, R., GIBA, Z. & DUAX, W. L. (1991). *Acta Cryst.* B**47**, 1010–1019.

LIFSON, S. & WARSHEL, A. (1969). *J. Chem. Phys.* **49**, 5116–5129.

LORAND, L. (1976). Editor. *Proteolytic Enzymes*, Part B, *Methods in Enzymology*, Vol. 45. New York: Academic Press.

MCDONALD, J. K. & BARRETT, A. J. (1986). *Mammalian Proteases*, Vol. 2. New York: Academic Press.

MAGNUS, V. (1987). In *Conjugated Plant Hormones, Structure, Metabolism and Function*, edited by K. SCHREIBER, H. R. SCHUETTE & G. SEMBDNER, pp. 31–40. Berlin: VEB Deutscher Verlag der Wissenschaften.

MAGNUS, V., HANGARTER, R. P. & GOOD, N. E. (1992). *J. Plant Growth Regul.* In the press.

MAGNUS, V., NIGOVIĆ, B., HANGARTER, R. P. & GOOD, N. E. (1992). *J. Plant Growth Regul.* **11**, 19–28.

MOLLAN, R. C., DONELLY, D. M. X. & HARMEY, M. A. (1972). *Phytochemistry*, **11**, 1485–1488.

MOTHERWELL, S., MURRAY-RUST, P., RAFTERY, J., ALLEN, F. & DOYLE, M. (1989). *GSTAT*89. Cambridge structural database integrated program for molecular geometry parameter calculations. Cambridge Crystallographic Data Centre, Univ. Chemical Laboratory, Cambridge, England.

NIGOVIĆ, B., KOJIĆ-PRODIĆ, B. & PUNTAREC, V. (1992). *Acta Cryst.* C**48**, 1079–1082.

NIGOVIĆ, B., KOJIĆ-PRODIĆ, B., PUNTAREC, V. & SCHAGEN, J. D. (1992). *Acta Cryst.* B**48**, 297–302.

ÖSTIN, A., BALDI, B., SUNDBERG, B., JENSEN, E., OLSSON, O., COHEN, J. D. & SANDBERG, G. (1990). *Physiol. Plant.* **79**(2), A27.

PARK, R. D. & PARK, C. K. (1987). *Plant Physiol.* **84**, 826–829.

SHELDRICK, G. M. (1983). *SHELX*77. Program for crystal structure determination. Univ. of Cambridge, England.

SHELDRICK, G. M. (1985). *SHELX*86. In *Crystallographic Computing* 3, edited by G. M. SHELDRICK, C. KRÜGER & R. GODDARD. Oxford Univ. Press.

SPEK, A. L. (1982). *The EUCLID Package*. In *Computational Crystallography*, edited by D. SAYRE, p. 528. Oxford: Clarendon Press.

TSURUMI, S. & WADA, S. (1986). *Plant Cell Physiol.* **27**, 1513–1522.

WANG, S. S., TAM, J. P., WANG, B. S. H. & MERRIFIELD, R. B. (1981). *Int. J. Pept. Protein Res.* **18**, 459–467.

WIELAND, T. & HÖRLEIN, G. (1955). *Liebigs Ann. Chem.* **591**, 192–199.